Cephalosporin-3'-diazeniumdiolate NO-donor prodrug PYRRO-C3D enhances azithromycin susceptibility of Non-typeable *Haemophilus influenzae* biofilms

Samuel A Collins[a,b], Michael J Kelso[c], Ardeshir Rineh[c], Nageshwar R Yepuri[c], Janice Coles[a], Claire L Jackson[a], Georgia D Halladay[a], Woolf T Walker[a,b], Jeremy S Webb[b,d], Luanne Hall-Stoodley[e], Gary J Connett[a,b], Martin Feelisch[a,b], Saul N Faust[a,b,f], Jane SA Lucas[a,b]#*, Raymond N Allan[a,f]*

[a]Clinical and Experimental Sciences, Faculty of Medicine and Institute for Life Sciences, University of Southampton, Southampton, UK

[b]Southampton NIHR Respiratory Biomedical Research Unit, University Hospital Southampton NHS Foundation Trust, Southampton, UK

[c]Illawarra Health and Medical Research Institute, School of Chemistry, University of Wollongong, Wollongong, NSW, Australia

[d]Centre for Biological Sciences, University of Southampton, Southampton, UK

[e]Department of Microbial Infection and Immunity, Centre for Microbial Interface Biology, College of Medicine, The Ohio State University, Columbus, Ohio, USA

[f]Southampton NIHR Wellcome Trust Clinical Research Facility, University Hospital Southampton NHS Foundation Trust, Southampton, UK

*Denotes equal contribution

Running Head: PYRRO-C3D enhances NTHi biofilm antibiotic susceptibility.

#Corresponding Author. Jane SA Lucas, Tel: +44-(0)23-8120-6160, E-mail: jlucas1@soton.ac.uk

ABSTRACT

Objectives: PYRRO-C3D is a cephalosporin-3-diazeniumdiolate nitric oxide (NO)-donor prodrug designed to selectively deliver NO to bacterial infection sites. The objective of this study was to assess the activity of PYRRO-C3D against non-typeable *Haemophilus influenzae* (NTHi) biofilms and examine the role of NO in reducing biofilm-associated antibiotic tolerance.

Methods: The activity of PYRRO-C3D on *in vitro* NTHi biofilms was assessed through CFU enumeration and confocal microscopy. NO release measurements were performed using an ISO-NO probe. NTHi biofilms grown on primary ciliated respiratory epithelia at an air-liquid interface were used to investigate the effects of PYRRO-C3D in the presence of host tissue. Label-free LC/MS proteomic analyses were performed to identify differentially expressed proteins following NO treatment.

Results: PYRRO-C3D specifically released NO in the presence of NTHi, while no evidence of spontaneous NO release was observed when the compound was exposed to primary epithelial cells. NTHi lacking β-lactamase activity failed to trigger NO release. Treatment significantly increased the susceptibility of *in vitro* NTHi biofilms to azithromycin, causing a log-fold reduction in viability ($p<0.05$) relative to azithromycin alone. The response was more pronounced for biofilms grown on primary respiratory epithelia, where a 2-log reduction was observed ($p<0.01$). Label-free proteomics showed that NO increased expression of sixteen proteins involved in metabolic and transcriptional/translational functions.

Conclusions: NO release from PYRRO-C3D enhances the efficacy of azithromycin against NTHi biofilms, putatively via modulation of NTHi metabolic activity. Adjunctive therapy with NO mediated through PYRRO-C3D represents a promising approach for reducing biofilm-associated antibiotic tolerance.

KEYWORDS

Haemophilus influenzae, biofilm, antibiotic resistance, nitric oxide, proteomics

1. INTRODUCTION

Non-typeable *Haemophilus influenzae* (NTHi) plays a major role in a number of chronic lung diseases, including chronic obstructive pulmonary disease, the fourth largest cause of mortality worldwide [1], and cystic fibrosis, where early childhood infection leads to an environment within the lung that is more susceptible to infection by *Pseudomonas aeruginosa* [2]. NTHi is also the predominant early coloniser in primary ciliary dyskinesia (PCD), another genetic chronic lung disease characterised by a lack of mucociliary clearance, chronic lung infection and lung function decline [3,4].

Persistence of NTHi infection is often associated with biofilm formation, with NTHi biofilms being implicated in a number of clinical settings including formation on middle ear epithelium during chronic otitis media [5], chronic rhinosinusitis [6], chronic obstructive pulmonary disease (COPD) sputum [7], and lower respiratory tract diseases [8]. The biofilm phenotype enables bacteria to evade the host immune response, benefit from increased antibiotic tolerance, and subsequently develop antibiotic resistance through horizontal gene transfer [9]. Exopolysaccharide matrix formation by biofilm bacteria may also restrict the diffusion of antibiotics into biofilms and prevent ingress of immune cells [10]. Increased expression of efflux pumps and β-lactamases have also been shown to contribute to increased tolerance. It is the change to a metabolically dormant phenotype, however, that potentially plays the most important role, rendering antibiotics that target cell division ineffective [11]. Biofilm formation in NTHi has been associated with the reduced metabolic activity typical of that observed in other bacterial species, with preserved ability to respond to stress [12]. As well as clinical isolates from a range of diseases having the ability to form *in vitro* biofilms [8], NTHi has also been shown to form biofilms on cultured respiratory epithelial surfaces with decreased antibiotic susceptibility [13,14]. NTHi biofilms also exhibit quorum signalling that is characteristic of other respiratory biofilm formers such as *P. aeruginosa* [15]. Whilst *P. aeruginosa* is the most widely studied biofilm forming respiratory

pathogen, many differences exist with NTHi. For example, *P. aeruginosa* biofilms form within mucus *in vivo* [16] rather than attached to the epithelial surface as NTHi biofilms do [5,6,13,14]. Also, cyclic-di-GMP seems to play a pivotal role in the *P. aeruginosa* biofilm life cycle under the control of guanylate cyclases and phosphodiesterases [17], however NTHi genome sequencing shows no domains coding for these enzymes [18].

Bacteria within biofilms can be triggered by various external factors to revert to a planktonic single cell state, a process that not only facilitates propagation and re-colonisation elsewhere within the host but also renders the bacteria more susceptible to antibiotics [10]. Development of a therapeutic approach that induces dispersal or reverses the metabolically dormant phenotype is therefore an attractive approach for improving antibiotic effectiveness in the treatment of biofilm-associated infections.

Nitric oxide (NO) is a ubiquitous signalling molecule that plays a wide range of biological roles in both prokaryotes and eukaryotes. Low dose NO has been shown to signal a dispersal response in biofilms formed by a number of bacterial species, including *P. aeruginosa*, *Escherichia coli*, *Serratia marcascens*, *Staphylococcus aureus*, and also multi-species biofilms [19-21]. However, NO also plays a number of important roles in the human host, meaning that administration of spontaneous NO donors as drugs would likely elicit undesirable side effects, particularly through alterations in circulatory dynamics [22-24]. To address this we have developed a novel class of targeted NO prodrugs (cephalosporin-3'-diazeniumdiolates) that are composed of a diazeniumdiolate (NONOate) NO-donor attached to the 3'-position of first generation cephalosporins. This innovative drug class was designed to selectively release the NONOate following cleavage of the β-lactam ring by bacterial β-lactamases, thereby targeting NO delivery directly to the site of infection [25] (Figure 1a). We hypothesised that treatment of NTHi biofilms with a cephalosporin-3'-diazeniumdiolate (i.e. PYRRO-C3D K+ salt, Figure 1a) would signal a return to a planktonic phenotype, thereby increasing NTHi sensitivity towards conventional antibiotics. We investigated the activity of

PYRRO-C3D, both alone and in combination with azithromycin, on biofilms formed *in vitro* and on primary respiratory epithelia grown at an air-liquid interface. High-throughput label-free proteomic analyses were performed to provide mechanistic insights into the role of NO in NTHi biofilms.

2. MATERIALS AND METHODS

2.1 Ethics

Local and national R&D and ethical approvals were obtained (Southampton and South West Hampshire Research Ethics 06/Q1704/105 and 07/Q1702/109).

2.2 Bacterial strains and growth conditions

NTHi strain HI4 was isolated from the sputum of a PCD patient. HI5 and HI6 were from nasal swabs of healthy children participating in a nasal carriage study. All experiments were performed using strain HI4 unless stated otherwise. HI4 and HI6 were β-lactamase producing strains, whilst HI5 lacked β-lactamase activity. Strains were subcultured onto Colombia agar with chocolated horse blood (CBA; Oxoid, U.K.) and grown at 37 ^{o}C and 5% CO_2. Colonies were resuspended in brain-heart infusion (BHI) broth (Oxoid, U.K.) supplemented with 10 μg/mL hemin and 2 μg/mL nicotinamide adenine dinucleotide.

2.3 Planktonic experiments

Flat-bottomed 96-well culture plates (Fisher Scientific, U.K.) were inoculated with ~1.0 x 10^7 mid-exponential NTHi grown in supplemented BHI. 10 mM PYRRO-C3D (in DMSO) was diluted in supplemented BHI and added to wells at final concentrations of 1 - 200 μM, with supplemented BHI used as an untreated control. Cultures were incubated at 37 ^{o}C and 5% CO_2 for 24 h. Absorbance (OD_{595}) was measured using an EZ Read 400 spectrophotometer (Biochrom; n=3).

2.4 In vitro biofilm experiments

Untreated polystyrene 6-well tissue culture plates (Corning Incorporated, U.S.A.) were inoculated with ~2.0 x 10^8 mid-exponential NTHi grown in supplemented BHI. Plates were incubated at 37 ^{o}C and 5 % CO_2 for 72 h and media replaced with fresh supplemented BHI daily. Biofilms were then washed twice with Hanks' Balanced Salt Solution (HBSS) to remove unattached cells before being treated with 10 nM - 100 µM PYRRO-C3D, 50 µM each of carboxy-PTIO (cPTIO), DEA/NO, clavulanate and cephaloram, and 4 mg/mL azithromycin for 2 hours at 37 ^{o}C and 5 % CO_2. Biofilms were washed twice then resuspended in 1 mL HBSS, vortexed, then serial diluted before being spot plated onto CBA and incubated at 37 ^{o}C and 5% CO_2. For confocal imaging, biofilms were grown on 35 mm untreated glass bottom CELLview culture dishes (Greiner Bio One, U.K.) and prepared as above. Following treatment, biofilms were stained with a Live/Dead BacLight bacterial viability kit (Life Technologies, U.S.A.) as per manufacturer's instructions and examined using a Leica SP8 Laser confocal scanning microscope (LCSM) with inverted stand under a 63x oil immersion lens. Sequential scanning was performed using 1 µm sections and the images analysed using Comstat 2.0 software [26].

2.5 Epithelial cell co-culture experiments

Nasal epithelial cells were obtained from healthy volunteers, cultured through two passages, then placed on 12 mm transwells (0.4 µm pore size) as previously described [27]. Once confluent, apical media was removed and the cells fed at the baso-lateral surface every 48 h. A minimum of 4 weeks after ciliation, trans-epithelial resistance was measured to confirm an intact epithelial surface [28]. NTHi in MEM containing HEPES without glutamine (ThermoFisher, U.K.) were applied to the apical surface of the epithelial cells at an MOI of 100:1. Co-cultures were grown for 72 h at 37 oC and 5% CO2 with the media changed every

24 h. Both the apical and baso-lateral surfaces were washed with HBSS prior to treatment. Co-cultures were treated with compounds and processed for CFU enumeration as before. Transwell membranes were removed, processed as previously described [29], and remaining biofilms imaged using an FEI Quanta 250 scanning electron microscope.

2.6 Nitric oxide measurements

Nitric oxide release from 50 µM PYRRO-C3D in phosphate buffered saline (PBS) was measured using an ISO-NO probe (World Precision Instruments, U.S.A.) as per the manufacturer's instructions. PYRRO-C3D was activated through addition of *Bacillus cereus* penicillinase (10 units, Sigma, U.K.) and NO release recorded over 130 minutes. NO release from PYRRO-C3D in the presence of mid-exponential NTHi cells was measured for 15 mins before quenching the reaction with 50 µM clavulanate (β-lactamase inhibitor). For epithelial cell co-culture measurements, 750 µL PBS was added to the apical surface and the probe inserted. Baseline NO release was measured for 30 mins before activating PYRRO-C3D through addition of 10 units of *B. cereus* penicillinase.

2.7 Proteomic analysis

An alternative NO-donor (sodium dinitroprusside, SNP) was used in place of PYRRO-C3D to characterise the response of NTHi biofilms to NO, without being confounded by any activity arising from the β-lactam component of PYRRO-C3D [30]. Untreated and 50 µM SNP treated *in vitro* NTHi4 biofilms were resuspended in 1 mL HBSS and washed twice by centrifugation at 10,000 xg for 5 mins at 4 ^{o}C. The supernatant was discarded, the pellet resuspended in digestion buffer containing 4 M guanidine hydrochloride, 10 mg/mL lysozyme, and 100 mM triethylammonium bicarbonate (TEAB) prepared in HBSS, and incubated at 37 ^{o}C for 30 mins. Samples were bead beaten with 0.1 mm zirconium oxide beads at 50 Hz for 5 minutes, centrifuged at 3,000 xg for 2 mins at room temperature, and the supernatants filter

sterilized through 0.22 µm polyethersulfone membranes to remove any remaining intact cells. Samples were precipitated overnight in 100% ethanol at -20 ^{o}C, centrifuged at 12,000 xg for 5 mins at 4^{o}C, and resuspended in 100 mM TEAB with 0.1% Rapigest SF surfactant (Waters, U.K.). Protein solutions were heat treated at 80 ^{o}C for 10 mins and then briefly vortexed. DTT (in 100 mM TEAB) was added to a final concentration of 2.5 nM then heat treated at 60 ^{o}C for 10 mins. After cooling, the solution was spun at 10,000 xg and iodoacetamide was added at a final concentration of 7.5 mM before incubating at room temperature for 30 mins in the dark. Protein samples were digested in trypsin solution overnight at 37 ^{o}C. Trifluoroacetic acid was added to a final concentration of 0.5% and the mixtures incubated for 30 minutes at 37 ^{o}C, before being centrifuged at 13,000 xg for 10 mins. The supernatant was lyophilised and resuspended in 200 mM ammonium formate with 100 fmol of enolase as internal standard.

2.7.1 Mass spectrometry of NTHi biofilm protein samples

Peptide separations were performed using a nanoAcquity UPLC system (Waters, U.K.). For the first dimension separation, 1.0 µL of the peptide digest was injected onto a Symmetry C18, 180µm x 20mm trapping cartridge (Waters, U.K.). After 5 min washing of the trap column, peptides were separated on a 75 µm i.d. x 250 mm, 1.7 µm BEH130 C18, column (Waters, U.K.) using a linear gradient of 5 to 40% B (buffer A = 0.1% formic acid in H_2O, buffer B = 0.1% formic acid in acetonitrile) over 90 min with a wash to 85% B at a flow rate of 300 nL/min. All separations were automated, performed on-line and sprayed directly into the nanospray source of the mass spectrometer. MS experiments were all performed using a Waters G2-S Synapt HDMS mass spectrometer operating in MS^{e} mode. Data were acquired from 50 to 2000 *m/z* with ion mobility enabled using alternate low and high collision energy (CE) scans. Low CE was 5V and elevated, ramped from 20-40V. The lock mass (Glu-

fibrinopeptide, $(M+2H)^{+2}$, *m/z* = 785.8426) was infused at a concentration of 100 fmol/µL at 300 nl/min and spectra acquired every 13 seconds.

2.7.2 Identification of proteins from MS spectra

The raw mass spectra were processed using ProteinLynx Global Server Ver 3.0 (enabled through Symphony pipeline software, Waters, U.K.) to generate a reduced charge state and de-isotoped precursor lists, with associated product ion mass lists. These mass lists were searched against the *H. influenzae* strain 3655 UniProt protein sequence (downloaded June 2016). A maximum of one missed cleavage was allowed for tryptic digestion and the allowed variable modification was set to contain oxidation of methionine. Carboxyamidomethylation of cysteine was set as a fixed modification.

2.8 Statistical analysis

Statistical analyses were performed using GraphPad version 6.04 and unpaired t-tests. Data reported with a significance ≤0.05 were considered statistically different. Analysis of identified proteins was corrected for multiple analysis using a false discovery rate (FDR) of 5%. Proteins that were either >1.5 or <0.7 fold changed following NO treatment were analysed using the Kyoto Encyclopaedia of Genes and Genomes (KEGG) [31,32] to identify over-represented biological pathways.

3. RESULTS

3.1 PYRRO-C3D elicits a direct antibacterial effect on planktonic but not biofilm NTHi

Prior to treatment of NTHi, NO release from PYRRO-C3D was first confirmed following chemical activation by the β-lactamase enzyme penicillinase. Activation of 50 µM PYRRO-C3D resulted in rapid release of NO, reaching a maximum concentration of ~600 nM over 14 minutes, which was followed by a gradual decline over a further 120 minutes (Figure 1b).

Treatment of planktonic NTHi cultures with increasing concentrations of PYRRO-C3D identified that concentrations >50 μM inhibited growth (Figure 2a). However, no reduction in biofilm viability was observed following PYRRO-C3D treatment at 10 nM - 100 μM over 2 hours (Figure 2b). Treatment of planktonic NTHi with 50 μM PYRRO-C3D released between 48 and 90 nM NO over 15 minutes, with the signal being quenched following addition of the β-lactamase inhibitor clavulanate (Figure 2c).

3.2 PYRRO-C3D enhances NTHi biofilm susceptibility to azithromycin

Previous research has shown that NO treatment of biofilms formed by several bacterial species reduces their tolerance towards antibiotics [33,34]. Treatment of established 72 h NTHi biofilms with 4 mg/mL azithromycin produced a slight reduction in viable NTHi within the biofilm ($p=0.0019$; Figure 3a). Complete killing, however, was not achieved despite the planktonic MIC for this strain being 0.001 mg/mL (data not shown). Combined treatment with 4 mg/mL azithromycin and 50 μM PYRRO-C3D resulted in a significant increase in bacterial killing, where a log-fold reduction in viable cells was observed in the biofilm population ($p=0.0189$; Fig. 3a). COMSTAT analysis of the live biofilm population following confocal imaging indicated that azithromycin alone had little impact on the viable biomass, whilst combined treatment with PYRRO-C3D produced a significant reduction ($p=0.0064$; Figure 3b). Notably, this reduction occurred despite a slight but significant increase in the live biofilm population occurring following treatment with PYRRO-C3D alone (Figure 3b). This effect, however, does not appear to be mediated by biofilm dispersal as a significant drop in the viable supernatant population with PYRRO-C3D alone was observed ($p=0.0061$; Figure 3c). No difference between azithromycin treatment alone and combined PYRRO-C3D/ azithromycin was also observed ($p=0.0974$; Figure 3c). COMSTAT analysis also showed no significant difference in biofilm thickness across any of the treatments, suggesting a lack of biofilm dispersal (Figure 3d). Measurement of biofilm density, assessed by average diffusion

distance between live bacteria, revealed that PYRRO-C3D alone increased biofilm density, whereas treatment with azithromycin had no effect (Figure 4). Combination treatment with azithromycin did, however, rescind the increase in biofilm density observed when treating with PYRRO-C3D alone (Figure 4).

3.3 Response of NTHi biofilms to PYRRO-C3D is NO-mediated

Having established that PYRRO-C3D potentiates the activity of azithromycin against NTHi biofilms, experiments were next performed to examine whether the effect was NO-mediated. Treatment of biofilms with an equivalent concentration (50 μM) of the spontaneous NO-donor DEA/NO alone had no effect on biofilm viability ($p=1.08$; Figure 5a). In contrast to the PYRRO-C3D/azithromycin combination, no increase in antibiotic efficacy was observed when DEA/NO was co-administered with azithromycin ($p=0.56$; Figure 5a). Treatment with the NO-scavenger cPTIO nullified the increase in azithromycin susceptibility observed in the presence of PYRRO-C3D ($p=0.0001$), suggesting that the potentiation effect is NO-mediated but requires slower, more controlled release of NO than is achievable with DEA/NO (Figure 5b). Treatment with cephaloram, the parent 1st generation cephalosporin from which PYRRO-C3D is derived (but lacking an NO donor), also showed no effect on biofilm viability in the absence or presence of azithromycin, suggesting that the potentiation response with PYRRO-C3D does not arise from β-lactam-mediated antibacterial activity (Figure 5a). The β-lactamase inhibitor clavulanate abrogated the potentiation response, consistent with NO release from PYRRO-C3D requiring β-lactamases (Figure 5b). This finding was corroborated by the absence of potentiation observed when treating a non-β-lactamase producing strain (HI5) with PYRRO-C3D and azithromycin ($p=0.24$), whilst observing a strong effect with an alternative β-lactamase producing strain HI6 ($p<0.0001$; Figure 6).

3.4 PYRRO-C3D increases azithromycin susceptibility of NTHi biofilms grown on primary respiratory epithelial cells

PYRRO-C3D treatment of NTHi biofilms formed on primary respiratory ciliated epithelial cells at an air-liquid interface (ALI) was used to investigate whether the presence of human host cells affected the activity of the compound. Lack of NO release from PYRRO-C3D in the absence of NTHi cells was first confirmed, where NO release was detected only after introduction of β-lactamase (Figure 7a). Scanning electron microscopy (SEM) was used to confirm NTHi biofilm formation following 72 h co-culture before proceeding with compound treatments (Figure 7c). As observed in the *in vitro* NTHi-only biofilm model, treatment of the co-cultures with PYRRO-C3D alone had no effect on viability ($p=0.41$) and treatment with azithromycin alone resulted in a log-fold reduction ($p=0.0007$). When used in combination, azithromycin and PYRRO-C3D produced a significant 2-log-fold reduction in viability relative to controls ($p=0.0026$; Figure 7b).

3.5 Nitric oxide treatment regulates protein expression in NTHi biofilms

Similar to *Streptococcus pneumoniae*, NTHi lacks proteins possessing the GGDEF, EAL and HD-GYP domains, which are important in the turnover of the secondary messenger cyclic-di-GMP (c-di-GMP) in response to NO-signals [35]. Label-free proteomic analyses were therefore performed to probe the mechanism by which NO affects NTHi biofilms. In total, 277 proteins were identified and 127 were expressed in both untreated and 50 μM SNP-treated biofilms. Of these proteins, 16 showed significantly increased expression (5% FDR) following SNP treatment and were primarily involved in either metabolic or transcriptional/translational processes (Table 1). KEGG pathway analysis of all proteins showing increased expression (>1.5 fold change) identified significant enrichment of ribosome pathways (34 proteins, FDR $1.2\text{x}10^{-28}$) and glycolysis/gluconeogenesis (9 proteins, FDR $1.55\text{x}10^{-5}$).

Uniprot code	Protein name	gene	Ratio treated/untreated
A0A0H3PBJ4	Glucose-specific PTS system enzyme IIA component*	crr	24.15
A0A0H3PK54	Lipoprotein (D-methionine uptake)*	metQ	21.52
A0A0H3PBW8	Phosphoglycerate kinase*	pgk	21.00
A0A0H3PFB4	DNA-directed RNA polymerase subunit alpha*	rpoA	16.33
A0A0H3PJ51	2,3-bisphosphoglycerate-dependent phosphoglycerate mutase*	gpmA	13.37
A0A0H3PG63	Elongation factor G*	fusA	12.96
A0A0H3PMV3	Pyruvate kinase*	pykA	11.85
A0A0H3PI75	Inosine-5'-monophosphate dehydrogenase*	guaB	11.41
A0A0H3PCZ6	L-lactate dehydrogenase*	lldD	10.50
A0A0H3PF36	ATP synthase subunit β	atpD	9.97
A0A0H3PLN7	Pyridoxal 5'-phosphate synthase subunit*	pdxS	9.15
A0A0H3PLM6	Pyruvate dehydrogenase E1 component*	aceE	8.25
A0A0H3PG47	Chaperone protein ClpB	clpB	7.89
A0A0H3PC20	NAD nucleotidase	nucA	6.99
A0A0H3PFF9	Long-chain fatty acid transport protein	OMPp1	6.09
A0A0H3PF51	CTP synthetase	pyrG	5.75

Table 1. Differentially expressed proteins in *in vitro* NTHi biofilms following SNP (50 μM) treatment. 5% false discovery rate (FDR), *=significant at 1% FDR.

4. DISCUSSION

NTHi, a common commensal in the upper respiratory tract, is an opportunistic pathogen responsible for localised and chronic lung infections associated with lung diseases. Biofilm formation by NTHi has been identified as playing a key role in both colonisation and disease, and contributes to ineffective antibiotic treatment [30]. NO has been shown to signal a dispersal response in several biofilm-forming species, rendering the released bacteria susceptible to antibiotics [19-21]. The ubiquitous nature of this molecule in human physiology, however, means that clinical implementation of non-specific NO treatments with, for example, gaseous NO or spontaneous NO-donors, could result in many side effects [22-

24]. Cephalosporin-3'-diazeniumdiolates like PYRRO-C3D, designed to target NO release specifically to bacterial infection sites, present a promising solution to this problem. Our findings indicate that PYRRO-C3D released low concentrations of NO upon contact with NTHi and that this release is specifically triggered by β-lactamases, as evidenced by the cessation of NO release in the presence of the β-lactamase inhibitor clavulanate. These data, and the lack of NO release when PYRRO-C3D was applied to respiratory epithelial cells in the absence of NTHi, demonstrates the specificity of the prodrug activation by bacterial cells, an attribute that would likely reduce the risk of NO-mediated side effects *in vivo*.

Regulation of the intracellular secondary messenger c-di-GMP plays a pivotal role in controlling both biofilm formation and dispersal, with increased levels promoting formation through increased aggregation, extracellular matrix and adhesin production, and reduced levels signalling a dispersal response [35-37]. C-di-GMP levels are regulated by diguanylate cyclases (containing GGDEF domains) that are responsible for its synthesis, and phosphodiesterases (containing HD-GYP and EAL domains) that catalyse degradation [37]. Increased activity of these phosphodiesterases has been linked to specific external triggers such as nutrient deprivation, hypoxia and NO [19,38-40]. A putative NO-sensing domain linked to both GGDEF and EAL domains, termed the NO-induced biofilm dispersal locus A (NbdA) [40], could be responsible for these downstream effects. However, it is unlikely that these mechanisms operate in *Haemophilus* spp. as genome-wide sequencing of NTHi (Rd KW20), *Haemophilus ducreyi, Haemophilus parainfluenzae* and *Haemophilus parasuis* indicates a lack of proteins possessing GGDEF, EAL or HD-GYP domains [18]. Our data support this since low concentrations of NO did not appear to reduce the number of viable cells remaining in biofilms following PYRRO-C3D treatment. However, our proteomic data suggest that an alternative signalling pathway may be involved.

Proteomic analyses comparing untreated and NO-treated NTHi biofilms demonstrated increased expression of sixteen proteins involved in metabolic or

transcriptional/translational processes. This was confirmed by KEGG pathway analysis of all differentially expressed proteins, which showed over-representation of ribosome and glycolysis/gluconeogenesis pathways. A similar response was recently observed in *Streptococcus pneumoniae* biofilms, where low dose NO modulated both translation and metabolism [33]. This is particularly interesting given that *S. pneumoniae* also lacks the GGDEF, EAL, and HD-GYP domain-containing proteins associated with the c-di-GMP pathway. It is possible that this is because both species inhabit the same nasopharyngeal niche, which not only provides an environment with limited nutrient availability, but also one with low levels of NO produced by epithelial cells [41]. Of particular interest was the increased expression of the D-methionine binding lipoprotein MetQ following NO treatment, an amino acid that has previously been shown to play a role in dispersal of *P. aeruginosa, S. auerus* and *Staphylococcus epidermidis* biofilms [42,43]. Interestingly, MetQ is also linked to a number of iron chelation/transporter proteins. It is known that iron can interfere with *P. aeruginosa* biofilm formation by inhibiting genes associated with biofilm formation, whilst SapF mediates heme utilisation and is involved in both biofilm persistence and coordination [44,45]. NO treatment of *E. coli* has also been shown to inhibit a global regulator (fur) that uses iron as a co-factor, affecting a wide range of metabolic processes such as the stress response and iron metabolism [46] and has been implicated in NTHi virulence [47].

While several studies have shown that NO-mediated dispersal of biofilms reduces antibiotic tolerance [19-21], the regulation of pneumococcal biofilm metabolism was recently shown to provide an alternative mechanism for reducing tolerance [33]. As PYRRO-C3D increases the susceptibility of NTHi biofilms to treatment with azithromycin, it is possible that a similar mechanism to that observed in pneumococcus is also responsible for reduction in tolerance observed here. Abrogation of the potentiation effect in the presence of the β-lactamase inhibitor clavulanate and the NO-scavenger cPTIO, in addition to the lack of response with cephaloram, confirmed that the response to PYRRO-C3D was indeed NO-

mediated. It is worth noting that treatment of a strain lacking β-lactamase activity failed to potentiate the activity of azithromycin, suggesting that PYRRO-C3D would likely be effective only against NTHi biofilms capable of β-lactamase production.

Observing a significant improvement in azithromycin efficacy when used alongside PYRRO-C3D but not in the presence of an equivalent concentration of the spontaneous NO donor DEA/NO suggests a bacteria-targeted NO-donor such as PYRRO-C3D would be more effective in the treatment of biofilm-associated infections. Whilst the half-life of DEA/NO is around 90 seconds, the release of NO from PYRRO-C3D continues for up to 120 minutes, suggesting that slow but sustained release is beneficial. Moreover, it was particularly noteworthy that NTHi biofilm susceptibility to combined PYRRO-C3D and azithromycin treatment was even more pronounced when co-cultured on primary epithelial cells – a more physiologically relevant model of biofilm infections in the respiratory tract.

5. CONCLUSION

In conclusion, this study has shown that the novel NO-donor prodrug PYRRO-C3D is effective in specifically targeting NO release to β-lactamase producing NTHi biofilms, and that through modulation of metabolic activity, the compound potentiates the antibacterial activity of azithromycin. This effect is not seen in the absence of β-lactamase production. PYRRO-C3D used in combination with azithromycin thus warrants further investigation as a potential treatment for chronic, biofilm-based NTHi infections.

Acknowledgments

We would like to thank the Southampton Biomedical Imaging Unit for their support in biofilm imaging, and Paul Skipp at the Southampton Centre for Proteomic Research for his support in the proteomic analyses. We would also like to thank Stuart Clarke at the

University of Southampton, Department of Clinical & Experimental Sciences, for provision of the non-typeable *Haemophilus influenzae* strains used in this study.

Funding:

MJK acknowledges funding from Australian Cystic Fibrosis Research Trust (ACFRT, 2014).

Transparency Declarations

None to declare

References

1. Halbert RJ, Natoli JL, Gano A, Badamgarav E, Buist AS, Mannino DM. Global burden of COPD: systematic review and meta-analysis. *Eur Respir J* 2006; **28**: 523-32.
2. Ramsey KA, Ranganathan S, Park J, Skoric B, Adams AM, Simpson SJ, Robins-Browne RM, Franklin PJ, de Klerk NH, Sly PD, Stick SM, Hall GL, Arest CF. Early respiratory infection is associated with reduced spirometry in children with cystic fibrosis. *Am J Respir Crit Care Med* 2014; **190**: 1111–6.
3. Alanin MC, Nielsen KG, von Buchwald C, Skov M, Aanaes K, Hoiby N, Johansen HK. A longitudinal study of lung bacterial pathogens in patients with primary ciliary dyskinesia. *Clin Microbiol Infect* 2015.
4. Rogers GB, Carroll MP, Zain NMM, Bruce KD, Lock K, Walker W, Jones G, Daniels TWV, Lucas JS. Complexity, temporal stability, and clinical correlates of airway bacterial community composition in primary ciliary dyskinesia. *J Clin Microbiol* 2013; **51**: 4029-35
5. Hall-Stoodley L, Hu FZ, Gieseke A, *et al.* Direct detection of bacterial biofilms on the middle-ear mucosa of children with chronic otitis media. *JAMA* 2006; **296**: 202–11.
6. Swords WE. Nontypeable Haemophilus influenzae biofilms: role in chronic airway infections. *Front Cell Infect Microbiol* 2012; **2**: 97.
7. Murphy TF, Kirkham C, Sethi S, Lesse AJ. Expression of a peroxiredoxin-glutaredoxin by Haemophilus influenzae in biofilms and during human respiratory tract infection. *FEMS Immunol Med Microbiol* 2005; **44**: 81–9.
8. Obaid NA, Jacobson GA, Tristram S. Relationship between clinical site of isolation and ability to form biofilms in vitro in nontypeable Haemophilus influenzae. *Can J Microbiol* 2015; **61**: 243–5.
9. Fux CA, Costerton JW, Stewart PS, Stoodley P. Survival strategies of infectious biofilms. *Trends Microbiol* 2005; **13**: 34–40.

10. Hall-Stoodley L, Stoodley P. Evolving concepts in biofilm infections. *Cell Microbiol* 2009; **11**: 1034–43.
11. Hoiby N, Bjarnsholt T, Givskov M, Molin S, Ciofu O. Antibiotic resistance of bacterial biofilms. *Int J Antimicro Agents* 2010; **35**: 322-332.
12. Post D, Held JM, Ketterer MR, *et al.* Comparative analyses of proteins from Haemophilus influenzae biofilm and planktonic populations using metabolic labeling and mass spectrometry. *BMC Microbiol* 2014; **14**: 329.
13. Starner TD, Zhang N, Kim G, Apicella MA, McCray PB. Haemophilus influenzae forms biofilms on airway epithelia: implications in cystic fibrosis. *Am J Respir Crit Care Med* 2006; **174**: 213–20.
14. Walker WT, Jackson CL, Coles J, *et al.* Ciliated cultures from patients with primary ciliary dyskinesia produce nitric oxide in response to Haemophilus influenzae infection and proinflammatory cytokines. *Chest* 2014; **145**: 668–9.
15. Unal CM, Singh B, Fleury C, *et al.* QseC controls biofilm formation of non-typeable Haemophilus influenzae in addition to an AI-2-dependent mechanism. *Int J Med Microbiol* 2012; **302**: 261–9.
16. Sriramulu DD, Lünsdorf H, Lam JS, Römling U. Microcolony formation: a novel biofilm model of Pseudomonas aeruginosa for the cystic fibrosis lung. *J Med Microbiol* 2005; **54**: 667–76.
17. Hickman JW, Tifrea DF, Harwood CS. A chemosensory system that regulates biofilm formation through modulation of cyclic diguanylate levels. *Proc Natl Acad Sci U S A* 2005; **102**: 14422–7.
18. Chou S-H, Galperin MY. Diversity of c-di-GMP-binding proteins and mechanisms. *J Bacteriol* 2015.
19. Barraud N, Hassett DJ, Hwang S-H, Rice SA, Kjelleberg S, Webb JS. Involvement of nitric oxide in biofilm dispersal of Pseudomonas aeruginosa. *J Bacteriol* 2006; **188**:

7344–53.

20. Barraud N, Storey M V, Moore ZP, Webb JS, Rice SA, Kjelleberg S. Nitric oxide-mediated dispersal in single- and multi-species biofilms of clinically and industrially relevant microorganisms. *Microb Biotechnol* 2009; **2**: 370–8.
21. Schlag S, Nerz C, Birkenstock TA, Altenberend F, Götz F. Inhibition of staphylococcal biofilm formation by nitrite. *J Bacteriol* 2007; **189**: 7911–9.
22. Ridnour LA, Thomas DD, Mancardi D, Espey MG, Miranda, KM, Paolocci N, Feelisch M, Fukuto J & Wink DA. The chemistry of nitrosative stress induced by nitric oxide and reactive nitrogen oxide species. Putting perspective on stressful biological situations. *Biol Chem* 2004; **385**:1-10.
23. Clutton-Brock J. Two cases of poisoning by contamination of nitrous oxide with higher oxides of nitrogen during anaesthesia. *Br J Anaesth* 1967; **39**: 388–92.
24. Jardeleza C, Thierry B, Rao S, Rajiv S, Driling A, Miljkovic D, Paramasavian S, James C, Dong D, Thomas N, Vreugde S, Prestidge CA, Wormald PJ. An in vivo safety and efficacy demonstration of a topical liposomal nitric oxide donor treatment for Staphylococcus aureus biofilm-associated rhinosinusitis. *Transl Res* 2015; **166**: 683–92.
25. Barraud N, Kardak BG, Yepuri NR, Howlin RP, Webb JS, Faust SN, Kjelleberg S, Rice SA, Kelso MJ. Cephalosporin-3'-diazeniumdiolates: targeted NO-donor prodrugs for dispersing bacterial biofilms. *Angew Chem Int Ed Engl* 2012; **51**: 9057–60.
26. Heydron A, Nielsen AT, Hentzer M, Sternberg C, Givskov M, Ersboll BK, Molin S. Quantification of biofilm structures by the novel computer program COMSTAT. *Microbiology* 2000. **146:** 2395-407.
27. Hirst RA, Jackson CL, Coles JL, Williams G, Rutman A, Goggin PM, Adam EC, Pahe A, Evans HJ, Lackie PM, O'Callaghan C, Lucas JS. Culture of Primary Ciliary Dyskinesia Epithelial Cells at Air-Liquid Interface Can Alter Ciliary Phenotype but Remains a

494 Robust and Informative Diagnostic Aid. *PLoS One* 2014; **9**: e89675.
495 28. Denker BM, Nigam SK. Molecular structure and assembly of the tight junction. *Am J*
496 *Physiol* 1998; **274**: F1–9.
497 29. Allan RN, Skipp P, Jefferies J, Clarke SC, Faust SN, Hall-Stoodley L, Webb J.
498 Pronounced metabolic changes in adaptation to biofilm growth by Streptococcus
499 pneumoniae. *PLoS ONE* 2014; **9**:e107015.
500 30. Wu S, Li X, Gunawardana M, *et al.* Beta- Lactam Antibiotics Stimulate Biofilm
501 Formation in Non-Typeable Haemophilus influenzae by Up-Regulating Carbohydrate
502 Metabolism. *PLoS One* 2014; **9**: e99204.
503 31. Kanehisa M, Goto S. KEGG: kyoto encyclopedia of genes and genomes. *Nucleic Acids*
504 *Res* 2000; **28**: 27–30.
505 32. Kanehisa M, Sato Y, Kawashima M, Furumichi M, Tanabe M. KEGG as a reference
506 resource for gene and protein annotation. *Nucleic Acids Res* 2016; **44**: D457–62.
507 33. Allan RN, Morgan S, Brito-Mutunayagam S, Skipp P, Feelisch M, Hayes SM, Hellier W,
508 Clarke SC, Stoodley P, Burgess A, Ismail-Koch H, Salib RJ, Webb JS, Faust SN & Hall-
509 Stoodley L. Low concentrations of nitric oxide modulate *Streptococcus pneumoniae*
510 biofilm metabolism and antibiotic tolerance. *Antimicrob Agents Chemother* 2016;
511 **60**(4):276-280.
512 34. Barraud N, Kelso MJ, Rice SA, Kjelleberg S. Nitric oxide: A mediator of biofilm
513 dispersal with applications in infectious diseases. *Curr Pharm Des* 2015; **21**(1): 31-42.
514 35. Hickman JW, Tifrea DF, Harwood CS. A chemosensory system that regulates biofilm
515 formation through modulation of cyclic diguanylate levels. *Proc Natl Acad Sci U S A*
516 2005; **102**: 14422–7.
517 36. Lee VT, Matewish JM, Kessler JL, Hyodo M, Hayakawa Y, Lory S. A cyclic-di-GMP
518 receptor required for bacterial exopolysaccharide production. *Mol Microbiol* 2007;
519 **65**: 1474–84.

37. Caly D, Bellini D. Targeting Cyclic di-GMP Signalling: A Strategy to Control Biofilm Formation? *Curr Pharm Des* 2015; **21**: 12–24.
38. Rao F, Yang Y, Qi Y, Liang Z-X. Catalytic mechanism of cyclic di-GMP-specific phosphodiesterase: a study of the EAL domain-containing RocR from Pseudomonas aeruginosa. *J Bacteriol* 2008; **190**: 3622–31.
39. An S, Wu J, Zhang L-H. Modulation of Pseudomonas aeruginosa biofilm dispersal by a cyclic-Di-GMP phosphodiesterase with a putative hypoxia-sensing domain. *Appl Environ Microbiol* 2010; **76**: 8160–73.
40. Li Y, Heine S, Entian M, Sauer K, Frankenberg-Dinkel N. NO-induced biofilm dispersion in Pseudomonas aeruginosa is mediated by an MHYT domain-coupled phosphodiesterase. *J Bacteriol* 2013; **195**: 3531–42.
41. Collins SA, Gove K, Walker W, Lucas JSA. Nasal nitric oxide screening for primary ciliary dyskinesia: systematic review and meta-analysis. *Eur Respir J* 2014; **44**: 1589–99.
42. Sanchez CJ, Akers KS, Romano DR, Woodbury RL, Hardy SK, Murray CK, Wenke JC. D-amino acids enhance the activity of antimicrobials against biofilms of clinical would isolates of Staphylococcus aureus and Pseudomonas aeruginosa. *Antimicrob Agents Chemother* 2014; **58**: 4353-61.
43. Ramon-Perez ML, Diaz-Cedillo F, Ibarra JA, Torales-Cardena A, Rodriquez-Martinez S, Jan-Roblero J, Cancino-Diaz ME, Cancino-Diaz JC. D-amino acids inhibit biofilm formation in Staphylococcus epidermidis strains from ocular infections. *J Med Micro* 2014; **63**: 1369-76.
44. Musk DJ, Banko DA, Hergenrother PJ. Iron salts perturb biofilm formation and disrupt existing biofilms of Pseudomonas aeruginosa. *Chem Biol* 2005; **12**: 789–96.
45. Vogel AR, Szelestey BR, Raffel FK, *et al.* SapF-mediated heme-iron utilization enhances persistence and coordinates biofilm architecture of Haemophilus. *Front*

Cell Infect Microbiol 2012; **2**: 42.

46. D'Autreaux B, Touati D, Bersch B, Latour J-M, Michaud-Soret I. Direct inhibition by nitric oxide of the transcriptional ferric uptake regulation protein via nitrosylation of the iron. *Proc Natl Acad Sci* 2002; **99**: 16619–24.

47. Harrison A, Santana EA, Szelestey BR, Newsom DE, White P, Mason KM. Ferric uptake regulator and its role in the pathogenesis of nontypeable Haemophilus influenzae. *Infect Immun* 2013; **81**: 1221–33.

Figure 1. a) Structure of PYRRO-C3D and NO release mechanism following β-lactam ring cleavage by β-lactamase. **b)** NO release from PYRRO-C3D (50 μM in PBS) following activation with β-lactamase (penicillinase).

Figure 2. PYRRO-C3D elicits a direct antibacterial effect on planktonic NTHi. a) Planktonic NTHi growth in the presence of PYRRO-C3D measured by absorbance (OD_{600}; n=4) **b)** 72 h *in vitro* NTHi biofilm viability following 2 h treatment with PYRRO-C3D as measured by CFU enumeration (n=4). **c)** NO release from 50 μM PYRRO-C3D in the presence of planktonic NTHi. The signal was recorded over 15 mins before quenching with the β-lactamase inhibitor clavulanate (n=2).

Figure 3. PYRRO-C3D increases NTHi *in vitro* biofilm susceptibility towards azithromycin treatment. 72 h NTHi *in vitro* biofilms treated with 50 μM PYRRO-C3D and 4 mg/ml azithromycin, both individually and in combination, for 2 h were assessed for viability through **a)** CFU enumeration, and **b)** COMSTAT analysis of live stained bacteria (n=5). **c)** Viability of the supernatant population following treatment measured by CFU enumeration, and **d)** maximum biofilm thickness measured by confocal microscopy. *p≤0.05, **p<0.01,***p≤0.001.

Figure 4. PYRRO-C3D treatment increases NTHi biofilm density. Confocal images of NTHi biofilms treated with 50 μM PYRRO-C3D and 4 mg/ml azithromycin, both individually and in combination, for 2 h were processed using COMSTAT software to calculate the average diffusion distance between live bacteria within biofilms. *p≤0.05.

Figure 5. Response of NTHi biofilms to PYRRO-C3D is NO-mediated. Viability of 72 h *in vitro* NTHi biofilms following 2 h treatment with **a)** 50 μM DEA/NO, cephaloram and PYRRO-C3D, and **b)** 50 μM cPTIO and clavulanate, both individually and in combination with 4 mg/mL azithromycin for 2 h. Measurement of viability through CFU enumeration *p≤0.05.

Figure 6. NO release from PYRRO-C3D is dependent on NTHi β-lactamase production. Viability of 72h *in vitro* biofilms formed by β-lactamase producing (HI6) and non-β-lactamase

584 producing (HI5) NTHi isolates following treatment with 50 µM PYRRO-C3D and 4 mg/ml
585 azithromycin both individually and in combination for 2 h, as assessed by CFU enumeration
586 (n=5). **p≤0.01.

587 **Figure 7. PYRRO-C3D treatment increases azithromycin susceptibility of NTHi biofilms**
588 **grown on primary respiratory epithelial cells. a)** Measurement of NO release from 50 µM
589 PYRRO-C3D in presence of primary respiratory epithelial cells isolated from grown at air
590 liquid interface (ALI) before and after activation with 10 units of β-lactamase (penicillinase).
591 **b)** Viability of 72 h NTHi biofilms grown at an ALI on primary respiratory epithelial cells
592 following 2 h treatment with 50 µM PYRRO-C3D and 4 mg/mL azithromycin, both alone and
593 in combination, as assessed by CFU enumeration (n=5). **c)** SEM image of a 72 h NTHi biofilm
594 formed at an ALI on primary respiratory epithelial cells. Scale bar = 10 µM, *p≤0.05,
595 **p≤0.01.

596

597

598

a)

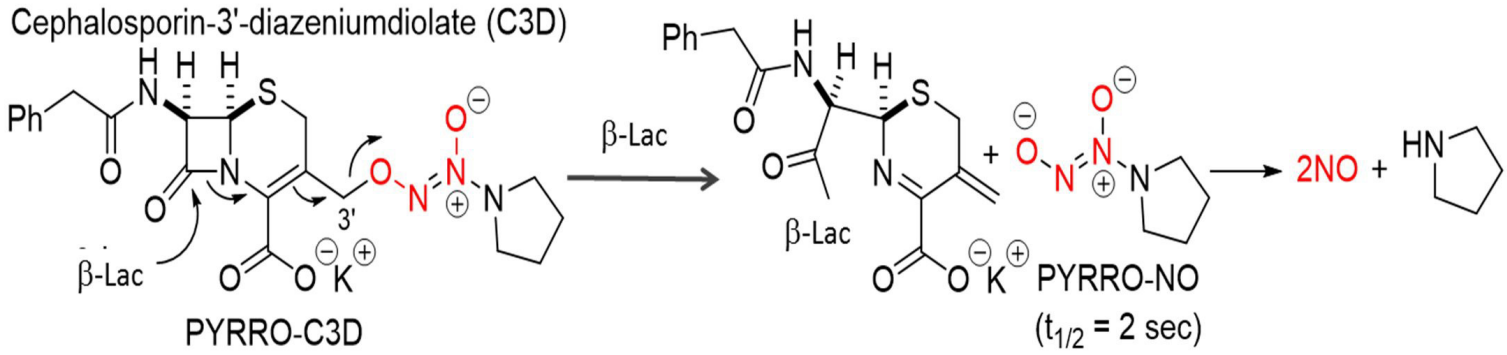

b)

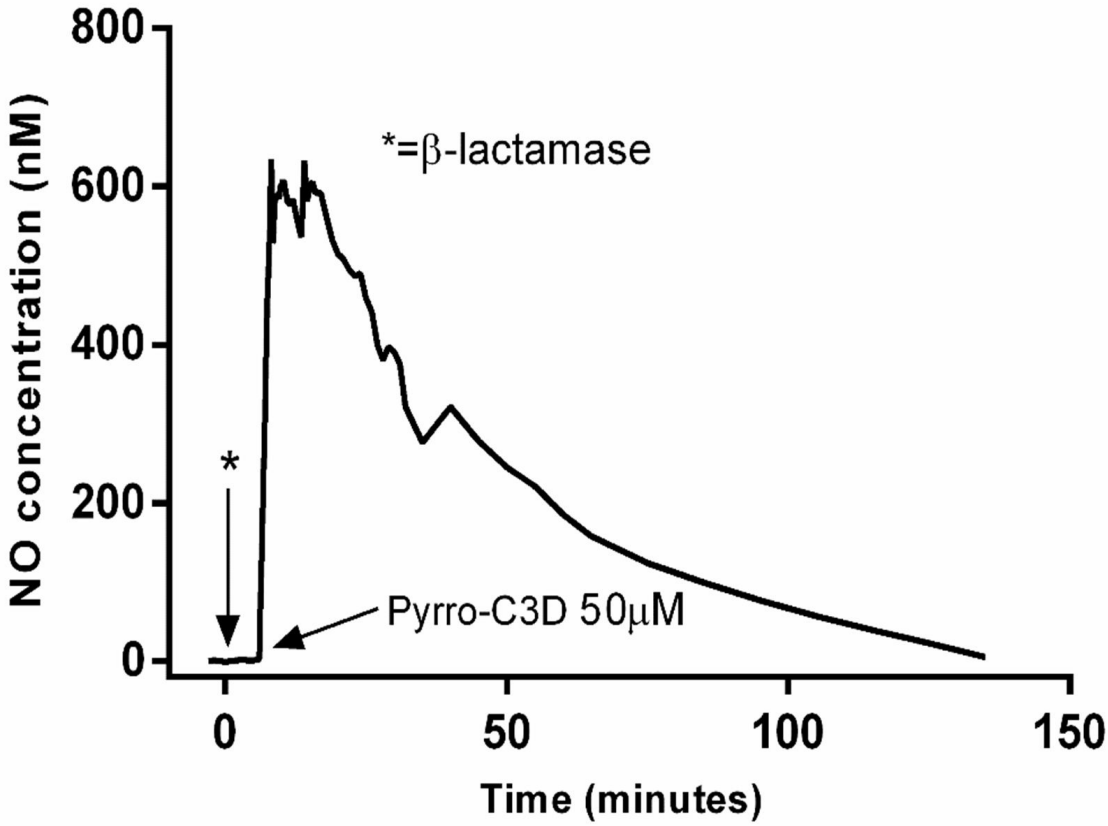

Figure 1. a) Structure of PYRRO-C3D and NO release mechanism following β-lactam ring cleavage by β-lactamase. **b)** NO release from PYRRO-C3D (50 mM in PBS) following activation with b-lactamase (penicillinase).

a)

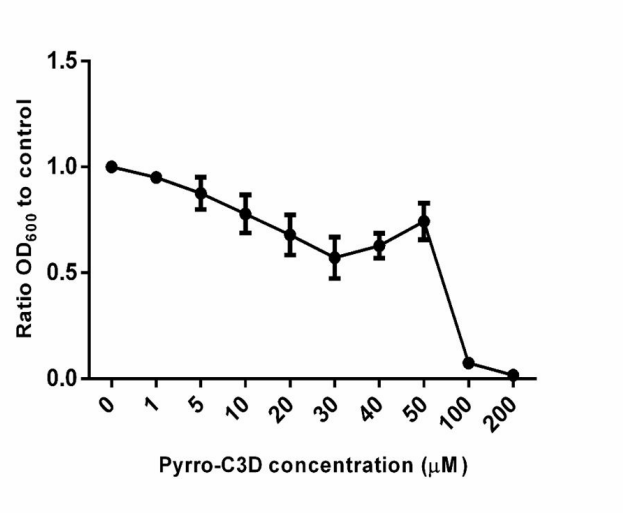

b)

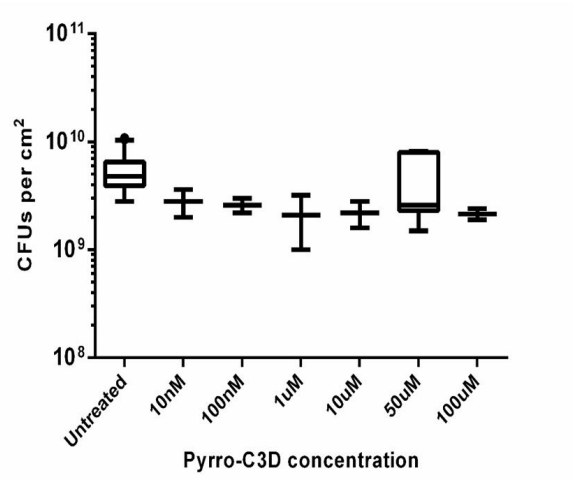

c)

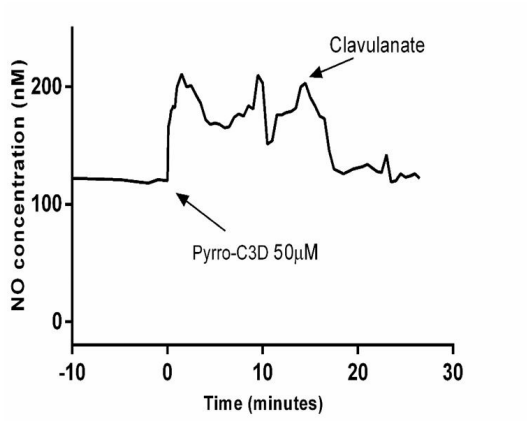

Figure 2. PYRRO-C3D elicits a direct antibacterial effect on planktonic NTHi. a) Planktonic NTHi growth in the presence of PYRRO-C3D measured by absorbance (OD_{600}; n=4) **b)** 72 h *in vitro* NTHi biofilm viability following 2 h treatment with PYRRO-C3D as measured by CFU enumeration (n=4). **c)** NO release from 50 µM PYRRO-C3D in the presence of planktonic NTHi. The signal was recorded over 15 mins before quenching with the β-lactamase inhibitor clavulanate (n=2).

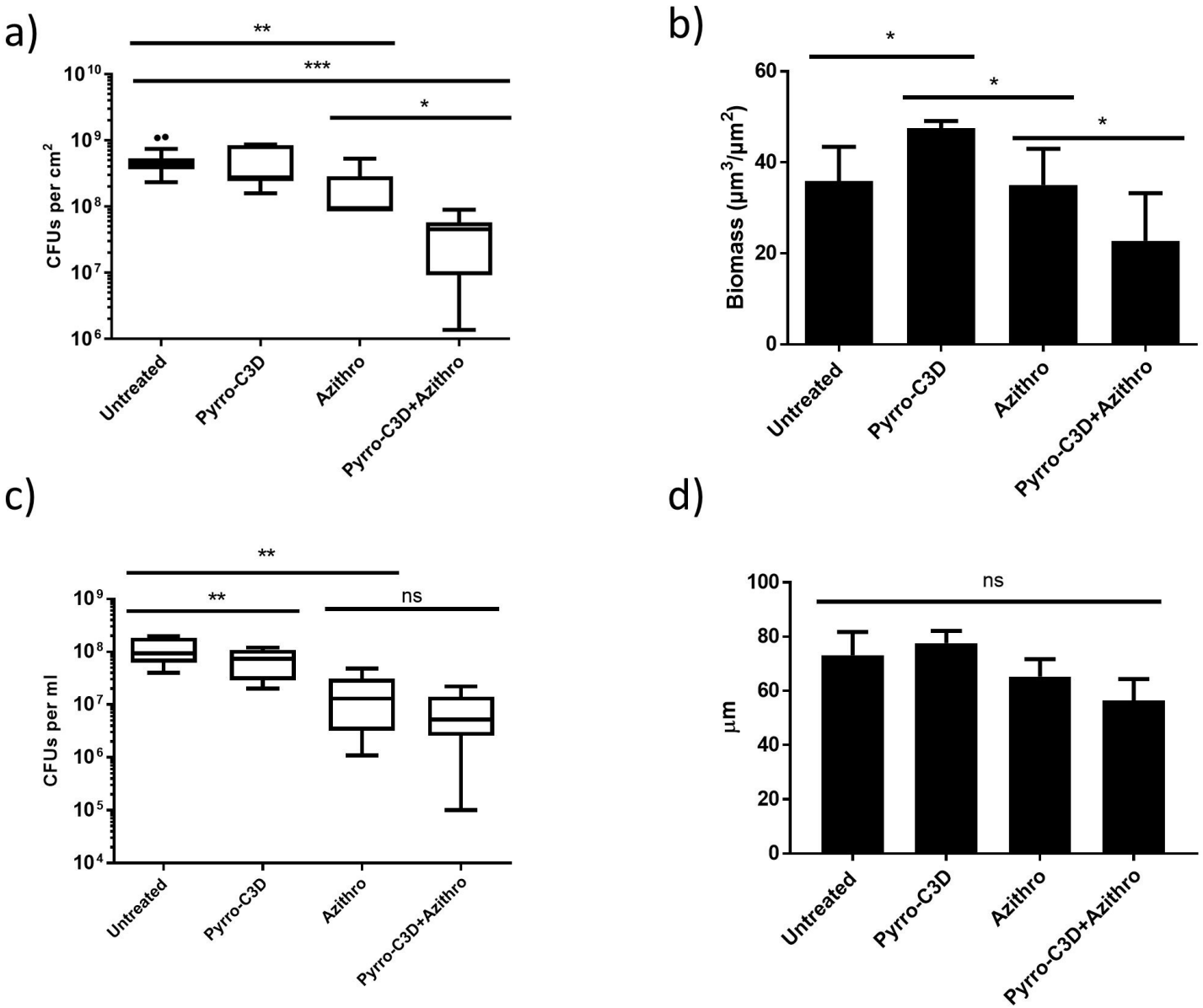

Figure 3. PYRRO-C3D increases NTHi *in vitro* biofilm susceptibility towards azithromycin treatment. 72 h NTHi *in vitro* biofilms treated with 50 µM PYRRO-C3D and 4 mg/ml azithromycin, both individually and in combination, for 2 h were assessed for viability through **a)** CFU enumeration, and **b)** COMSTAT analysis of live stained bacteria (n=5). **c)** Viability of the supernatant population following treatment measured by CFU enumeration, and **d)** maximum biofilm thickness measured by confocal microscopy. *p≤0.05, **p<0.01,***p≤0.001.

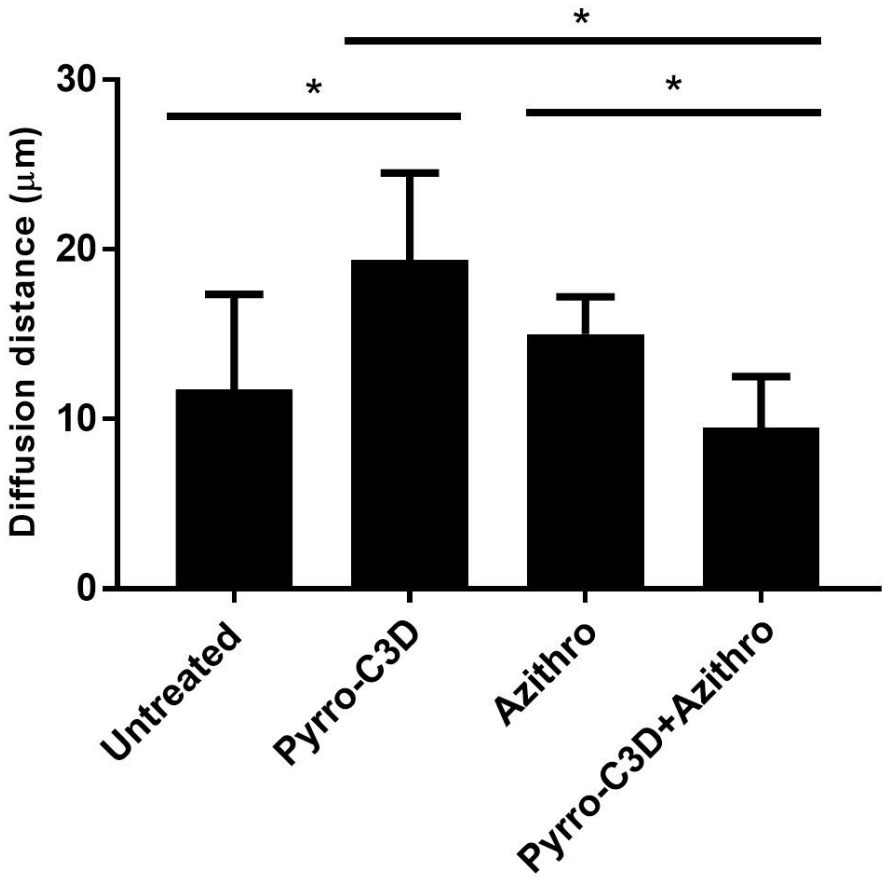

Figure 4. PYRRO-C3D treatment increases NTHi biofilm density. Confocal images of NTHi biofilms treated with 50 μM PYRRO-C3D and 4 mg/ml azithromycin, both individually and in combination, for 2 h were processed using COMSTAT software to calculate the average diffusion distance between live bacteria within biofilms. *p≤0.05.

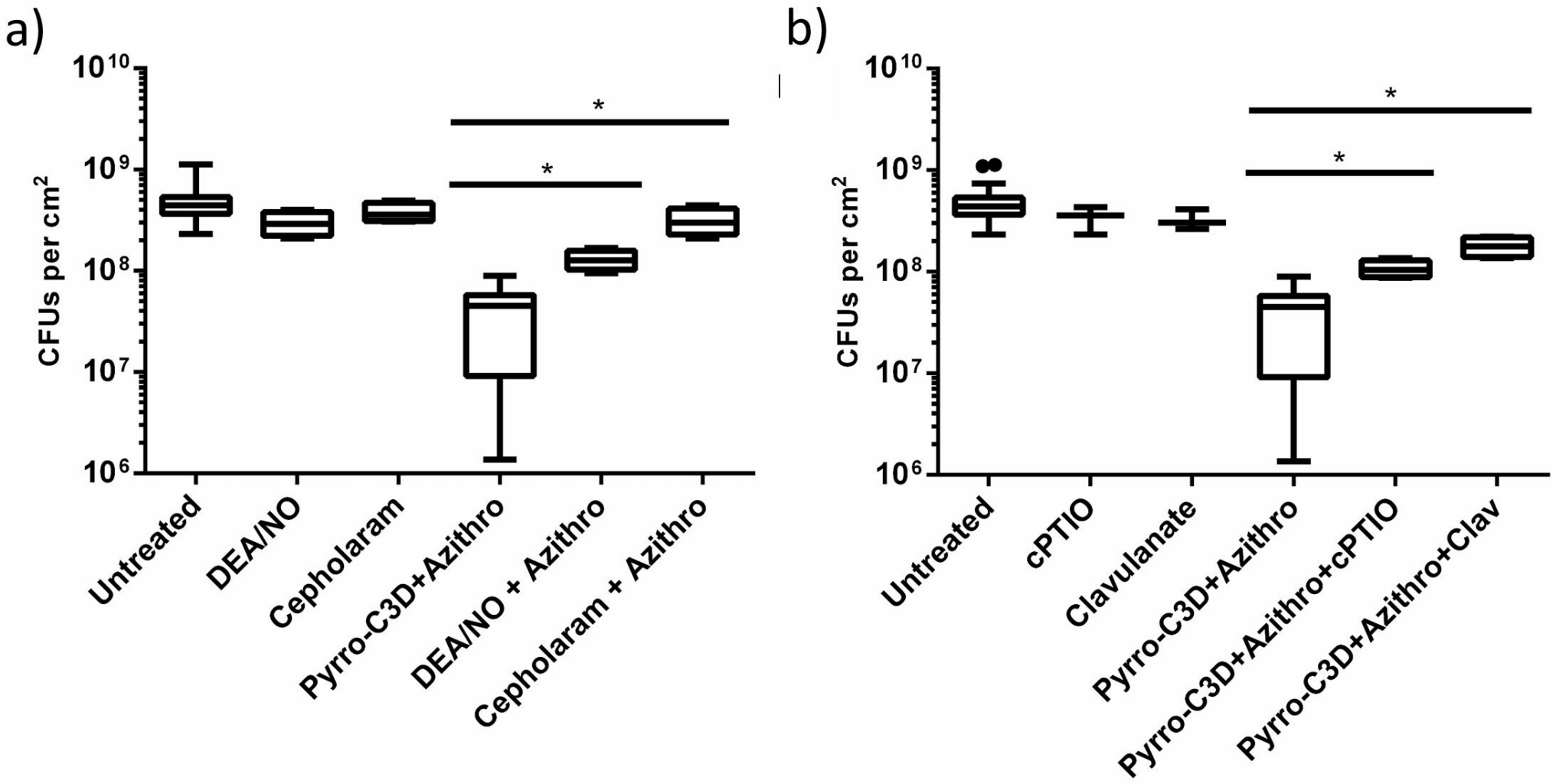

Figure 5. Response of NTHi biofilms to PYRRO-C3D is NO-mediated. Viability of 72 h *in vitro* NTHi biofilms following 2 h treatment with **a)** 50 µM DEA/NO, cephaloram and PYRRO-C3D, and **b)** 50 µM cPTIO and clavulanate, both individually and in combination with 4 mg/mL azithromycin for 2 h. Measurement of viability through CFU enumeration *p≤0.05.

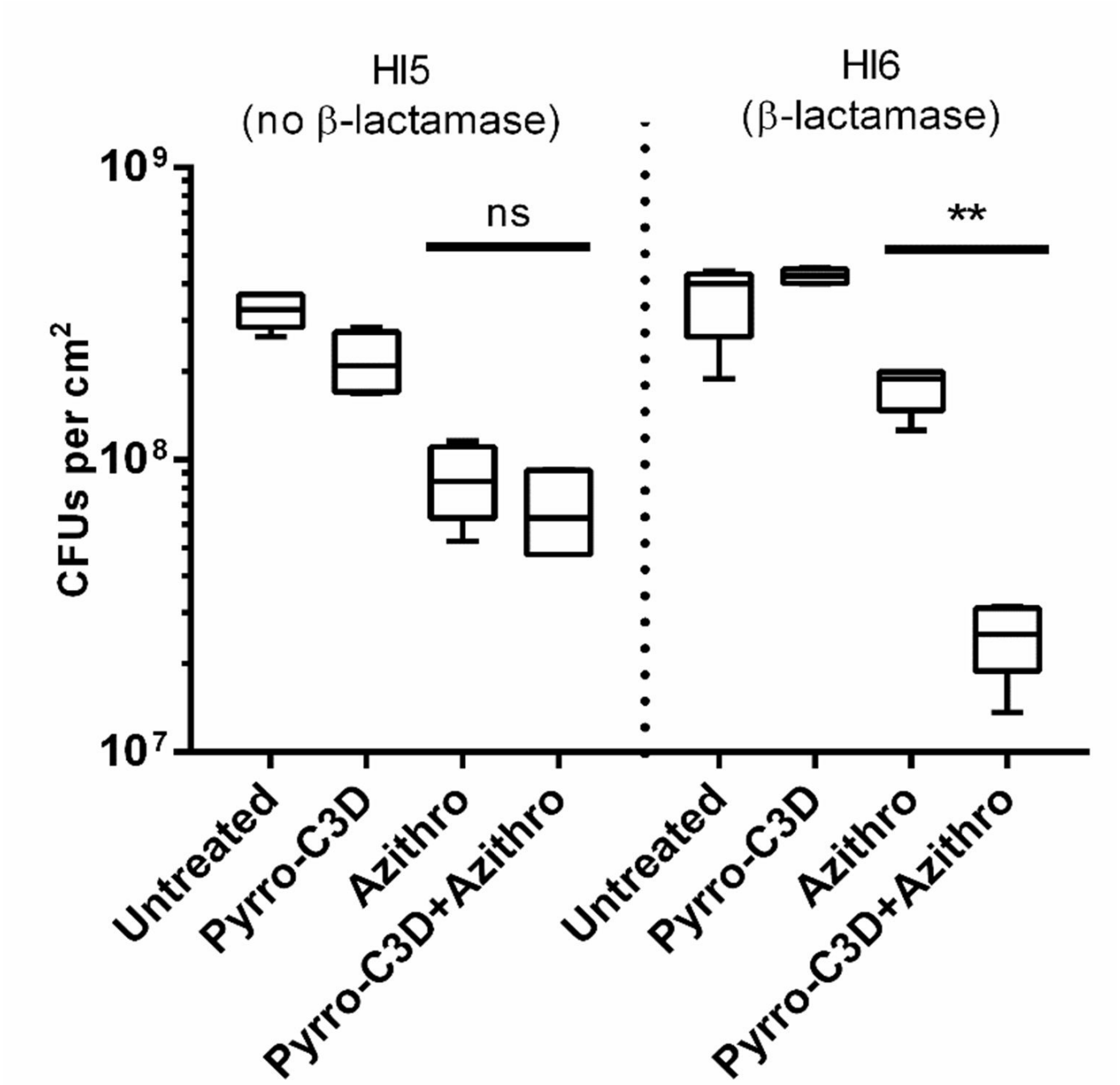

Figure 6. NO release from PYRRO-C3D is dependent on NTHi β-lactamase production. Viability of 72h *in vitro* biofilms formed by β-lactamase producing (HI6) and non-β-lactamase producing (HI5) NTHi isolates following treatment with 50 μM PYRRO-C3D and 4 mg/ml azithromycin both individually and in combination for 2 h, as assessed by CFU enumeration (n=5). **p≤0.01.

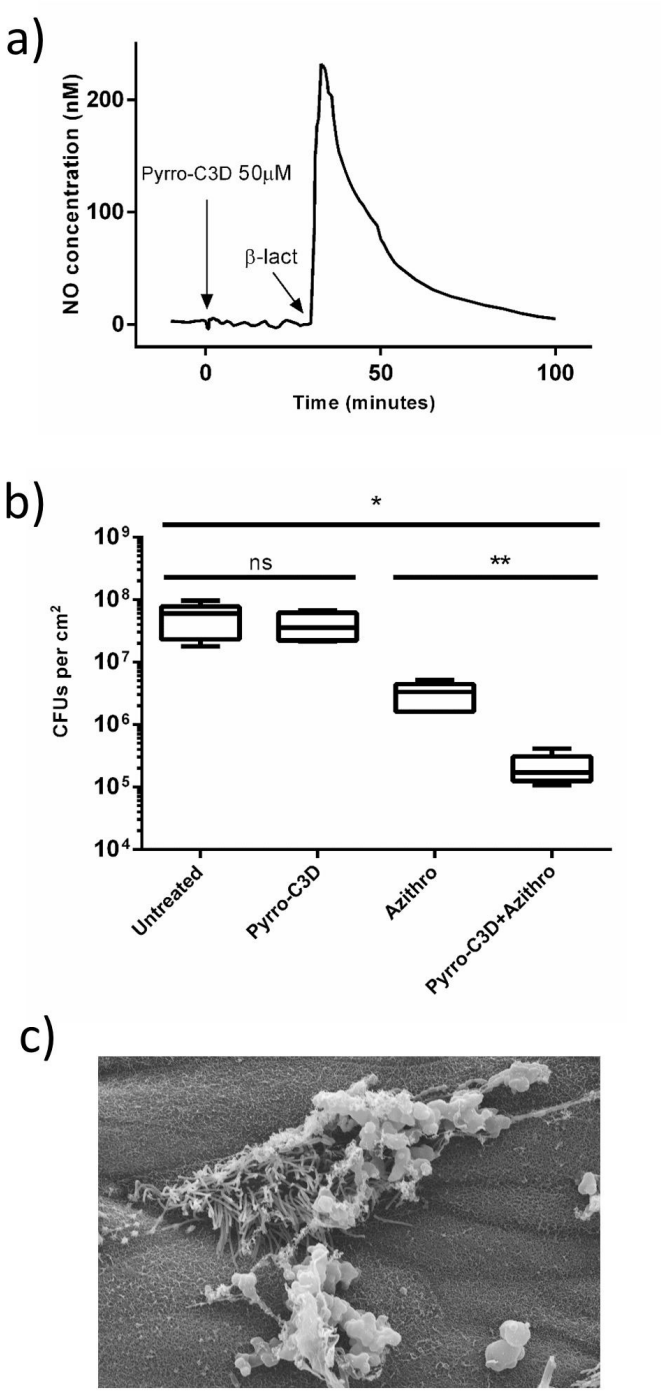

Figure 7. PYRRO-C3D treatment increases azithromycin susceptibility of NTHi biofilms grown on primary respiratory epithelial cells. a) Measurement of NO release from 50 μM PYRRO-C3D in presence of primary respiratory epithelial cells isolated from grown at air liquid interface (ALI) before and after activation with 10 units of β-lactamase (penicillinase). **b)** Viability of 72 h NTHi biofilms grown at an ALI on primary respiratory epithelial cells following 2 h treatment with 50 μM PYRRO-C3D and 4 mg/mL azithromycin, both alone and in combination, as assessed by CFU enumeration (n=5). **c)** SEM image of a 72 h NTHi biofilm formed at an ALI on primary respiratory epithelial cells. Scale bar = 10 μM, *p≤0.05, **p≤0.01.